Dual-Function Fibrous Co-Polypeptide Scaffolds for Neural Tissue Engineering

Tienli Ma, Shangchih Yang, Shyhchyang Luo, Weili Chen, Shulang Liao, and Weifang Su*

This paper reports dual-function (high cell attachment and cell viability) fibrous scaffolds featuring aligned fibers, displaying good biocompatibility and no cytotoxicity. These scaffolds are fabricated through the electrospinning of a co-polypeptide comprising molar equivalents of N_6-carbobenzyloxy-L-lysine and γ-benzyl-L-glutamate, with the lysine moieties enhancing cell adhesion and the neural-stimulating glutamate moieties improving cell viability. These new scaffolds allow neural cells to attach and grow effectively without any special surface treatment or coating. Pheochromocytoma (PC-12) cells grown on these scaffolds exhibit better neuronal activity and longer neurite length, relative to those grown on scaffolds prepared from their respective homo-polypeptides. When the scaffolds are partially hydrolyzed such that they present net positive charge and increased hydrophilicity, the cell viability and neurite growth both increase further. Accordingly, these novel co-polypeptide fibrous scaffolds have potential applications in neural tissue engineering.

1. Introduction

Nerve injury caused by disease, aging, trauma, and surgery can cause physical dysfunction and pain. Many strategies have been developed for nerve repair, including grafting and bridging of tubular techniques, end-to-end suturing of nerve stumps, and nerve autografting.[1,2] Nevertheless, these techniques can have several drawbacks, including loss of donor site, donor site morbidity, a need for multiple surgeries, non-specific incomplete reinnervation, and poor neurological recovery. Furthermore, suitable nerve collection sites and the length of available graft tissue might be limited.[3] Although allografts and xenografts are alternatives,[4] there remains a risk of disease transmission or a need for additional steps of immunosuppression to avoid rejection. Bioengineered grafts are, however, promising because the technology can evolve with new neural development strategies and insights into regeneration and regeneration mechanisms.[5]

Neural tissue engineering is a potential solution to nerve damage and disease. Here, nerves are cultured in vitro on biomimetic scaffolds and then transferred onto the damaged parts of nerves for regeneration.[6–8] Biocompatible scaffolds prepared through electrospinning can mimic the natural extracellular matrix (ECM) and accelerate neural tissue repair and regeneration when using bioactive molecules in the cell culture.[7] Furthermore, scaffolds with aligned fibers can mimic the topography of uninjured anatomical structures in the nerve and guide regenerative cells to grow and function in the direction of the fibers.[8] Fibrous scaffolds prepared from peptide-based materials are suitable for biomedical applications because they possess good biocompatibility, chemical diversity, and the ability to promote interactions between cells and substrates;[9–11] they have potential uses in, for example, regenerative medicine and tissue engineering, drug and gene delivery, and biosensing.[12–17] Among such peptide-based materials, poly(γ-benzyl-L-glutamate) (PBG) has been investigated extensively for tissue engineering because of its ease of chemical synthesis and because its glutamate units function as neural stimulators.[18–21] Glutamate is an important neurotransmitter in the central nervous system (CNS); it controls the subventricular zone and can regulate nerve regeneration, synaptogenesis, neural transmission, and neurogenesis.[22]

In our previous studies, scaffolds fabricated from glutamate based homo-polypeptide (PBG) exhibited higher biocompatibility, mechanical properties, scaffold stability, and longer neurite extension performance than those of the commonly known polycaprolactone (PCL) biopolymer.[18,23] Moreover, PBG polypeptide-aligned fibrous scaffolds exhibited excellent effects on both neural cells and retinal ganglion cells derived from human induced pluripotent stem cells (iPSCs).[21] Notably, PBG can regenerate

T. Ma, S. Luo, W. Chen, W. Su
Department of Materials Science and Engineering
National Taiwan University
Taipei, Da'an Dist. 106319, Taiwan
E-mail: suwf@ntu.edu.tw

S. Yang, S. Liao
Department of Ophthalmology
National Taiwan University College of Medicine
Taipei, Zhongzheng Dist. 100233, Taiwan

W. Chen, S. Liao
Department of Ophthalmology
National Taiwan University Hospital
Taipei, Zhongzheng Dist. 100225, Taiwan

W. Chen
Advanced Ocular Surface and Corneal Nerve Regeneration Center
National Taiwan University Hospital
Taipei, Zhongzheng Dist.100225, Taiwan

W. Su
Department of Materials Engineering
Ming Chi University of Technology
New Taipei City, Taishan Dist. 243303, Taiwan

The ORCID identification number(s) for the author(s) of this article can be found under https://doi.org/10.1002/mabi.202200286

corneal nerves in damaged corneas in the animal model.[24] All of the results indicated that glutamate-based polypeptide has a neurostimulatory effect on the growth of nerve cells which was not observed in PCL-based fibrous scaffolds. Furthermore, the glutamate based scaffolds display a synergistic effect with nerve growth factor (NGF) in terms of the capacity of differentiation which was not observed using PCL.[21–24] Upon hydrolysis of glutamate, the formation of glutamic acid can increase both the number of cell-recognizable ligands and the growth rate of neurites.[23] Because the hydrolyzed glutamate is negatively charged, it does, however, worsen the cell adhesion on the substrate.[25] The use of co-polypeptides can be a good approach toward obtaining desired combinations of properties for specific applications in tissue engineering.[26–29]

Ideally, functional scaffolds used in tissue engineering should ensure the dual functions of good cell attachment and good cell viability. Preferably, they should be easy to prepare from a single material. Herein, we report the development of dual-function fibrous scaffolds featuring aligned fibers that display good biocompatibility and no cytotoxicity. We fabricated them through electrospinning of a co-polypeptide comprising molar equivalents of N_6-carbobenzyloxy-L-lysine and γ-benzyl-L-glutamate. Here, the lysine moieties of the co-polypeptide enhanced cell adhesion, while the neural-stimulating glutamate moieties improved the cell viability. These new scaffolds allowed neural cells to attach and grow effectively without the need for surface treatment or coating. Pheochromocytoma (PC-12) cells grown on these scaffolds exhibited better neuronal activity and longer neurite length relative to those grown on scaffolds prepared from the respective homo-polypeptides. When we partially hydrolyzed the scaffolds to present positive charge and increase their hydrophilicity, both the cell viability and neurite growth increased further. This report is the first to describe positively charged co-polypeptide fibrous scaffolds with potential applications in neural tissue engineering.[30–33]

2. Experimental Section

2.1. Materials

The chemicals used for synthesis and fabrication were L-glutamic acid γ-benzyl ester (Sigma-Aldrich), N_ϵ-carbobenzyloxy-L-lysine (Sigma-Aldrich), triphosgene (Sigma-Aldrich), sodium (Sigma-Aldrich), ethyl acetate (EA; Acros), tetrahydrofuran (THF; Sigma-Aldrich), benzene (Sigma-Aldrich), methanol (Sigma-Aldrich), N,N-dimethylacetamide (DMAc; Sigma-Aldrich), acetone (Sigma-Aldrich), d-trifluoroacetic acid (Acros), ethyl ether (Macron), hexane (Uni-Onward, Taiwan), and 33 wt% hydrogen bromide (HBr) in acetic acid (Acros). The chemicals used for the cell experiments were Dulbecco's modified Eagle's medium high glucose (DMEM-HG; Gibco), Roswell Park Memorial Institute 1640 medium (RPMI-1640; Hyclone), DMEM/F12 medium (Gibco), phosphate-buffered saline (PBS; Sigma-Aldrich), Alamar Blue cell cytotoxicity assay (Thermofisher), fetal bovine serum (FBS; VWR Life Science Seradigm), horse serum (HS; Gibco), antibiotic antimycotic solution—penicillin/streptomycin/amphotericin B (PSA; Sigma-Aldrich), 0.25% trypsin protease (Simply), dimethyl sulfoxide (DMSO; Sigma-Aldrich), bovine serum albumin (BSA;

Uni-Onward), live/dead viability/cytotoxicity kit (Thermofisher), TOOLSmart RNA Extractor (Biotools), TOOLS Quick RT Kit (Biotools), SYBR Green 2X Master Mix (Kapa Biosystems), ECL Select Western Blotting Detection Reagent (Cytiva), nerve growth factor-2.5S from murine submaxillary gland (NGF; Sigma-Aldrich), formaldehyde (Acros Organics), 4,6-diamidino-2-phenylindole (DAPI; Sigma-Aldrich), phalloidin-tetramethyl rhodamine B isothiocyanate (phalloidin-TRITC; Sigma-Aldrich), anti-β-Tubulin III antibody (Abcam), anti-GAP43 antibody (Abcam), anti-SYN1 (Synapsin1) antibody (Sigma), anti-GAPDH antibody (Sigma), Alexa Fluor 488 goat anti-Mouse IgG (H+L) secondary antibody (Abcam), HRP-goat anti-mouse IgG (H+L) secondary antibody (Invitrogen), HRP-goat anti-rabbit IgG (H+L) secondary antibody (Invitrogen), and octyl phenol ethoxylate (Triton X-100; J. T. Baker).

2.2. Instruments and Equipment

The chemical structures of the synthesized co-polypeptides were determined using nuclear magnetic resonance (NMR) spectroscopy (Bruker; DPX400) and Fourier transform infrared (FTIR) spectroscopy (PerkinElmer; Spectrum 100). Their molecular weights were determined through gel permeation chromatography (GPC; Waters; Breeze 2), with N,N-dimethylformamide (DMF) containing 0.05 wt% LiBr as the mobile phase and polystyrene standards used to establish the calibration curve. Water contact angle analysis (Model 100SB, Sindatek) was used to measure the hydrophilicity of the fibrous scaffolds. The zeta potential of hydrolyzed co-polypeptide (0.01 wt% in water) was measured using dynamic light scattering (DLS; Brookhaven 90Plus nanoparticle size analyzer). The instruments used for the cell experiments included a centrifuge (Kubota; 2420), an incubator (ESCO; 81022), a thermostatic water bath (DSB500E, Digisystem), a laminar flow hood (ESCO; class II type A2), a 4°C refrigerator (SC122, Azotech), a −20 °C refrigerator (SCF-141K, Sanyo), an optical microscope (DMI3000 B; Leica), a confocal microscope (TCS SP5 II, Leica), and an absorbance microplate reader (ELx800, BioTek). Western blot images were acquired using a UVP BioSpectrum 810 and analyzed using Vision Works LS software (UVP). Real-time PCR was performed using a Bio-Rad CFX Connect instrument and analyzed using Bio-Rad CFX Connect Manager 3.1 software (Bio-Rad). Scanning electron microscopy (JSM-6510, JEOL) was performed to determine the fiber diameters of the various scaffolds and to characterize the morphologies of the neurite growth of 5-d differentiated PC-12 cells on the polypeptide scaffolds. Images of all scaffold fibers were magnified up to 3000× for measurements of their diameters; Table S1 (Supporting Information) summarizes the results. The polypeptide fibrous scaffolds were fabricated using an electrospinning system (Sunway Scientific Corporation).

2.3. Nomenclature

The following abbreviations are used throughout this study: poly(γ-benzyl-l-glutamate) (PBG); poly(N_6-carbobenzyloxy-L-lysine) (PCBZL); γ-benzyl glutamate-N-carboxyanhydride (BG-NCA); N_6-carbobenzyloxy-L-lysine-N-carboxyanhydride (CBZL-

ADVANCED
SCIENCE NEWS
www.advancedsciencenews.com

[M]acro-
molecular
Bioscience
www.mbs-journal.de

Table 1. Electrospinning parameters used to obtain polypeptide fibrous scaffolds.

Polypeptide	Concentration [wt%]	Mixed solvent [v/v]	Voltage [kV]	Flow rate [mL h^{-1}]
PBG	20	THF/DMAc = 6:4	20	5
PCBZL	20	DMAc/acetone = 5:5	20	5
5CBZL5BG	20	DMAc/acetone = 1:2	22	4.8

NCA); poly[(N_6-carbobenzyloxy-L-lysine)$_x$-co-(γ-benzyl-L-glutamate)$_\gamma$] (P((CBZL)$_x$-co-(BG)$_\gamma$)) (x:γ = 50:50% molar ratio, 5CBZL5BG); hydrolyzed P((CBZL)$_x$-co-(BG)$_\gamma$) became ((PCBZL)$_k$(PLL)$_l$)$_x$-co-((PBG)$_m$(PGA)$_n$)$_\gamma$ (5BL28-5BGA18).

2.4. Polypeptide Scaffolds

2.4.1. Preparation of Polypeptide Scaffolds

A 20 wt% polypeptide solution was prepared for electrospinning the 3D fibrous scaffolds throughout this study. Typically, the PBG polypeptide was dissolved in a cosolvent of THF and DMAc, and PCBZL and 5CBZL5BG were dissolved in a cosolvent of DMAc and acetone. The prepared polypeptide solution was poured into a 5-mL glass syringe fixed to a syringe pump. High voltage was applied to the needle tip; the aligned fibers were collected on cover slips (diameter: 12 mm) attached to the cylinder collector covered with aluminum foil; the speed of rotation was 3200 rpm. The distance between the collector and the needle was ≈15 cm. After completion of the electrospinning process, the fibrous scaffold was placed, together with the aluminum foil, in a vacuum oven and the residual solvent was evaporated at 40 °C overnight. **Table 1** lists the parameters of the electrospinning processes for the various polypeptides.

To isolate the scaffolds, the co-polypeptide scaffolds electrospun on the cover slip were immersed in 3-mm-diameter glass dishes containing HBr in water [20% (v/v), 1 mL] for 1 h at room temperature. The sample was removed, washed five times sequentially with water and ethyl ether, and then vacuum-dried at 40 °C overnight.

2.4.2. Characterization of the Alignment of Fibers in Polypeptide Scaffolds

The scaffolds with aligned fibers were prepared using an electrospinning equipment with a cylinder collector. The average % of fiber alignment in different scaffolds in this study was analyzed through Image J analysis of the SEM photos of scaffolds. The alignment of fibers was calculated from the angle changes between fibers and displayed as the distribution maps of orientation (alignment). Then, the % alignment (orientation) can be obtained through statistical calculation.

2.5. Biocompatibility of Polypeptide Scaffolds

2.5.1. Cytotoxicity Test—Live/Dead Assay

The scaffolds were soaked in PSA solution [1% in PBS (v/v)] and sterilized with UV light overnight prior to cell seeding. The

RPMI-1640 medium was treated with 10% (v/v) HS, 5% (v/v) FBS, and 1% (v/v) PSA prior to use. PC-12 cells were seeded on the polypeptide scaffolds at a cell density of 20 000 cells cm^{-2} in 24-well polystyrene (PS) cell culture plates. The PC-12 cells were cultured at 37 °C and 5% CO$_2$ for 5 d. The culture medium was renewed every 2 d. The culture medium was removed after 5 d and the scaffolds were washed with PBS. The cultured cells were then stained—with calcein-AM [0.05% in PBS (v/v)] for live cells and EthD-1 [0.2% in PBS (v/v)] for dead cells—at room temperature for 45 min. The staining solution was removed and the samples were washed with PBS. The cells were then ready for analysis using fluorescence optical microscopy.

2.5.2. Cell Viability Test—Alamar Blue Assay

The cell viability of the polypeptide scaffold was tested using an Alamar Blue assay, in which dark-blue nonfluorescent Resazurin interacted with NADH dehydrogenase in the granulosa glands of living cells to oxidize NADH/H$^-$ to NAD+/H$_2$O, while the dye was reduced to highly fluorescent pink reduced Resorufin. The reduction rate of the dye could be determined from the absorbance of visible light (at 570 and 600 nm), which correlated to the cell viability. The cell seeding procedure for the cell viability experiment was the same as that described for the Live/Dead assay. PC-12 cells were cultured in medium at 37 °C and 5% CO$_2$ for 1, 3, or 5 d. The culture medium was removed after 1 d and replaced with diluted Alamar Blue solution [10% in DMEM (v/v)], after the samples had been washed with PBS. The blank group was a well containing medium, but no cells. The cells were kept in an incubator at 37 °C/5% CO$_2$ for 5 h to react with the Alamar Blue reagent. The solutions in the 24-well plate were placed in another 96-well plate to measure the absorbances at 570 and 600 nm, using a microplate reader. After washing with PBS, the cells were kept culturing up to the third and fifth days; the procedure described for the first day was then used to determine the absorbances of the cultured cell solutions.

2.6. Characterization of Neural Differentiation of PC-12 Cell on Polypeptide Scaffolds

2.6.1. Fluorescent Staining of PC-12 Cells

Scaffolds were prepared on cover slips and PC-12 cells were seeded in the same way as described for the biocompatibility tests in Section 2.5. The PC-12 cells were seeded on the scaffolds at a density of 5000 cells cm^{-2}. NGF (100 ng mL^{-1}) was added to the cell culture medium after 1 d to induce neural differentiation. The differentiation medium was renewed every 2 d. After culturing for 5 d, the medium was removed and washed with PBS. The cells were fixed using formaldehyde solution [3.7% in PBS (v/v)] for 15 min and permeabilized using Triton-X 100 solution [1% in PBS (v/v)] for 10 min at room temperature. The PC-12 cells were stained for β3 tubulin with β3 tubulin antibody. The samples were washed with PBS and treated with β3 tubulin primary antibody diluted solution (1:200 in PBS) at 4 °C overnight. After the primary antibody solution was removed, the samples were washed with PBS and incubated with goat anti-mouse IgG

(H+L) cross-adsorbed secondary antibody diluted solution (1:200 in PBS) for 40 min at room temperature. After the secondary antibody solution had been removed and washed with PBS, the samples were stained for F-actin by phalloidin for 1 h and stained for nucleus by DAPI for 5 min. The samples were washed with PBS three times and observed under a fluorescence microscope.

2.6.2. Characterization of PC-12 Neurite Growth

Phalloidin labeling was used to measure the neurite length. The neurite length was measured from the cell body to the tip of the neurite, using Image J software. In each sample, the lengths of more than 120 neurites were measured. The alignment angles of the neurites were calculated from the changes in angle between the cell neurites and the aligned fibers, using Image J software; they are displayed as distribution maps. The neurite alignment was characterized in terms of the percentage of neurites having an angular orientation within ±15° of the 0–180° axis, determined through phalloidin labeling.

2.6.3. Western Blot Analysis of PC-12 Cells

The PC-12 cells were cultured on the PS plate and scaffolds and then collected after being treated with or without NGF for 5 d. The wells were first washed three times with sterile PBS and then the cells were lysed with ice-cold RIPA buffer. The procedure for Western blot analysis was performed as described previously by Shen et al.[34] In brief, collected proteins (30 μg) were blotted onto PVDF membranes and then incubated with anti-GAP43, anti-SYN1 (Synapsin1) and anti-GAPDH antibodies at 4 °C overnight. Next day, the membranes were blotted with secondary antibodies conjugated with horseradish peroxidase (HRP). The blots were developed using an ECL Select Western Blotting Detection Reagent (Cytiva). The bands were imaged using a UVP BioSpectrum 810 system.

2.6.4. RNA Extraction and Real-Time PCR Analysis of PC-12 Cells

The total RNA of the PC-12 cells that were subjected to the various culture conditions was isolated using a TOOLSmart RNA Extractor (Biotools), according to the manufacturer's instructions. The extracted RNAs were subjected to reverse transcription using a TOOLS Quick RT Kit (BIOTOOLS). The resulting cDNAs (100 ng/sample) were used as templates for real-time PCR analysis using a SYBR Green 2X Master Mix (Kapa Biosystems) and measured using a CFX Connect instrument (Bio-Rad). The relative amounts of the target genes GAP43 and SYN1 (Synapsin1) were normalized against the RNA levels of glyceraldehyde 3-phosphate dehydrogenase (GAPDH). The sequences of the primers for analysis were as follows:

GAP43-F: 5′-AGAAAGCAGCCAAGCTGAGGAGG-3′
GAP43-R: 5′-CAGGAGAGACAGGGTTCAGGTGG-3′
GAPDH-F: 5′-TGGCGCTGAGTACGTCGTG-3′
GAPDH-R: 5′-ATGGCATGGACTGTGGTCAT-3′
SYN1 (Synapsin1)-F: 5′-CAGGGTCAAGGCCGCCAGTC-3′
SYN1 (Synapsin1)-R: 5′-CACATCCTGGCTGGGTTTCTG-3′

2.7. PC-12 Cell Morphology on Polypeptide Scaffold

The morphologies of the PC-12 cells on the scaffolds were characterized using SEM. Scaffolds on cover slips were prepared and PC-12 cells were seeded in a same way as described for the biocompatibility tests in Section 2.5. PC-12 cells were seeded on the scaffolds at a density of 5000 cells cm^{-2} and culturing for 5 d. The PC-12 cells on the scaffolds were then fixed using glutaraldehyde solution [2.5% (v/v) in PBS] for 1 h at room temperature. The cells were soaked for 15 min in aqueous ethanol solutions of increasing concentrations (30%, 50%, 70%, 80%, and 90%, respectively). The cells were immersed in 95% ethanol (two times for 15 min each) and 99.5% ethanol (two times for 15 min each). Finally, the cells were kept in 99.5% ethanol until required for the vacuum drying process.

3. Results and Discussion
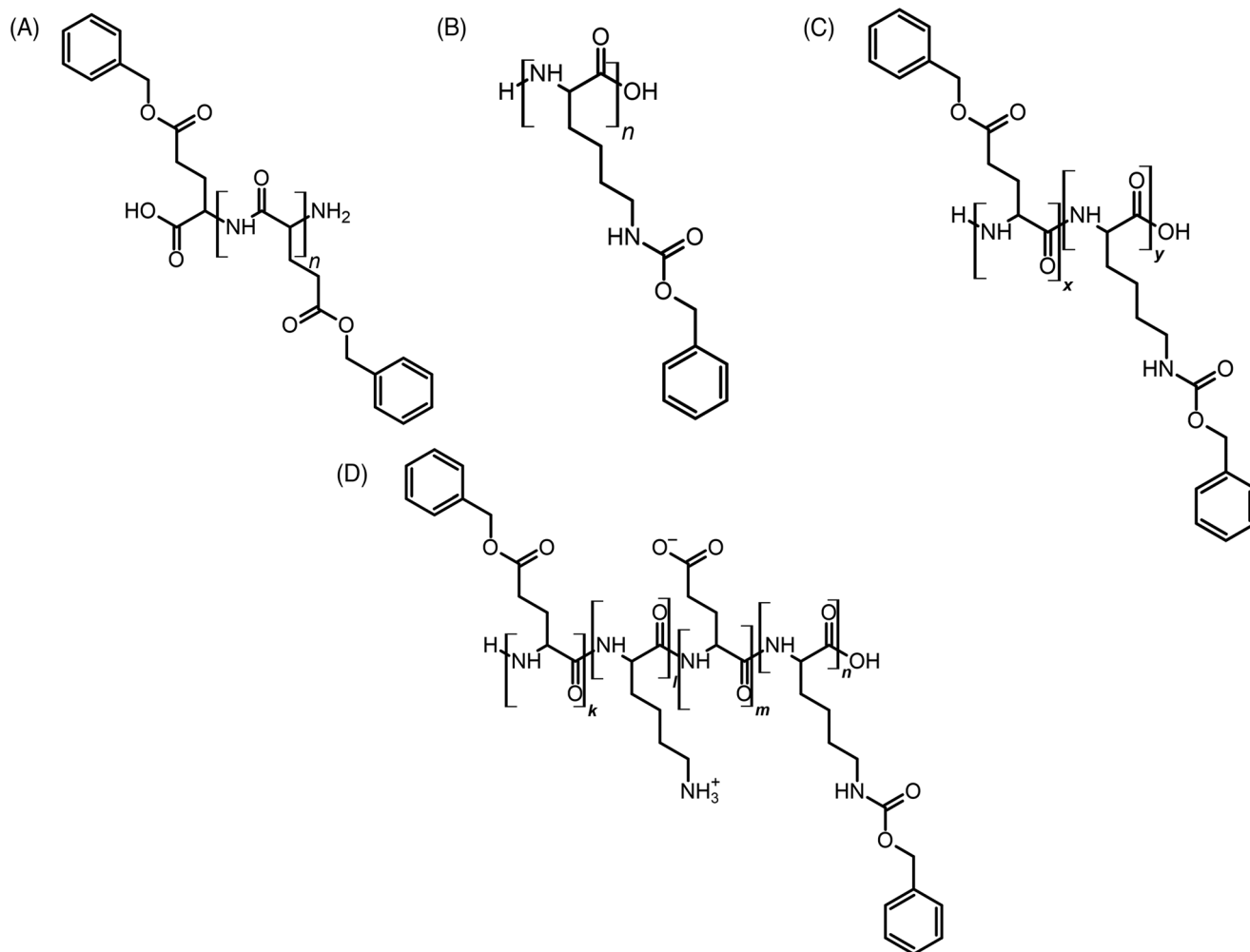
3.1. Characterization of Polypeptides

Homo-polypeptides and co-polypeptides were synthesized through ring-opening polymerization, according to procedures reported previously.[18,28] The monomer ratio of the co-polypeptide P((CBZL)$_x$-co-(BG)$_y$) was 5:5. The synthesis and characterization of homo-polypeptides and co-polypeptides are detailed in the Supporting Information. We used NMR and IR to confirm the chemical structures of synthesized products as shown in Figures S1–S4 (Supporting Information). **Figure 1** presents the chemical structures of the synthesized polypeptides.

We used GPC to determine the molecular weights of the various polypeptides; Figure S5 (Supporting Information) displays their GPC traces. The molecular weights of polypeptides were controlled in the range 600–700 kDa with polydispersity indexes in the range 1.0–1.3, to eliminate any effect of molecular weight on the properties of polypeptides, and for ease of electrospinning. **Table 2** summarized these values.

The 5CBZL5BG co-polypeptide was hydrolyzed with aqueous HBr to introduce positive charges. We determined the degree of hydrolysis from the degrees of deprotection of the protecting groups of the glutamic acid (Bn) and lysine (CBZ) moieties, as evaluated using FTIR spectroscopy (Figure S6, Supporting Information) according to the changes in peak height of the signals for the C=O groups of CBZ and Bn.[28] All of the calculated peaks were normalized with respect to the signal for the amide groups on the main chain of the co-polypeptide. We concluded that 28% of the CBZ units and 18% of the Bn units had been hydrolyzed. The hydrolyzed co-polypeptide is designated as ((PCBZL)$_k$(PLL)$_l$)$_x$-co-((PBG)$_m$(PGA)$_n$)$_y$ and abbreviated as 5BL28-5BGA18. Because the hydrolysis rate of CBZ was faster than that of Bn,[28] the co-polypeptide had a net positive charge arising from the lysine moieties, as confirmed through DLS zeta potential measurement at +31.87 mV (Figure S7, Supporting Information).

3.2. Fabrication and Characterization of Polymer Fibrous Scaffolds

We fabricated scaffolds containing aligned fibers to guide neural cell growth and differentiation. The polypeptide fibrous scaf-

**ADVANCED
SCIENCE NEWS**

www.advancedsciencenews.com

**Macro-
molecular
Bioscience**

www.mbs-journal.de

Figure 1. Chemical structures of different polypeptides. A) PBG, B) PCBZL, C) 5CBZL5BG, and D) 5BL28-5BGA18.

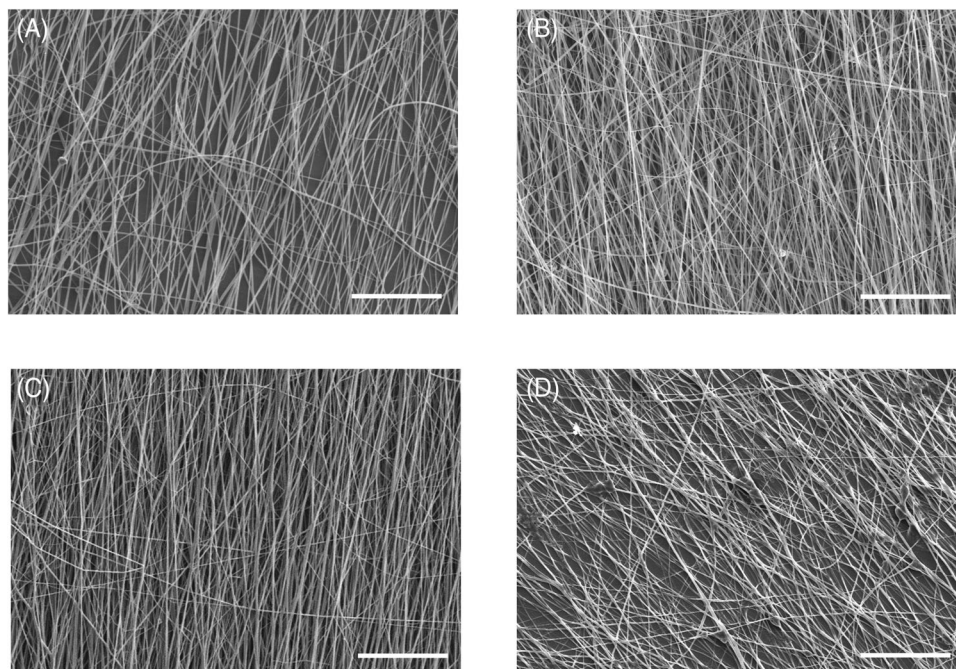**Table 2.** Characteristics of synthesized PBG, PCBZL, and 5CBZL5BG.

Polypeptide	MW [kDa]	PDI (M_w/M_n)	Yield [%]
PBG	683	1.24	90
PCBZL	640	1.16	86
5CBZL5BG	604	1.08	89

folds were collected on the cylinder collector during electrospinning, with the alignment of the fibers controlled by changing the concentration of the polypeptide solution, voltage, and flow rate. We controlled the diameter of the fibers to be in the approximate range 1.0–1.3 μm (Table S1 and Figure S8, Supporting Information) to ensure good cell attachment on the scaffold.[35] **Figure 2** displays SEM images of different polypeptide scaffolds made with aligned fibers. The polypeptide fibrous scaffolds had similar scaffold densities (PBG: 21 μg mm^{-3}; PCBZL: 24 μg mm^{-3}; 5CBZL5BG: 25 μg mm^{-3}; 5BL28-5BGA18: 25 μg mm^{-3}) to ensure similar culturing conditions in each case. We used Equation (S1) (Supporting Information) to calculate the polymer scaffold density. The 5BL28-5BGA18 scaffold was made by immers-

ing the 5CBZL5BG scaffold in aqueous HBr, without distorting the aligned fibers. Figure S9 (Supporting Information) reveals the orientations of the polypeptide fibrous scaffolds.

The hydrophilicity of a scaffold will affect its ability to mediate the adhesion of cells and, furthermore, its ability to differentiate cells. Polymer substrates having moderate hydrophilicity provide ideal environments for cell attachment.[36,37] We used water contact angle measurements to determine the hydrophilicity of our polypeptide scaffolds and to compare their hydrophilicities before and after modification. **Figure 3** reveals that the water contact angles of our polypeptide fibrous scaffolds were as follows: PBG, 122.7° ± 10.5°; PCBZL, 74.7° ± 10.4°; 5CBZL5BG, 89.9° ± 4.9°; 5BL28-5BGA18, 81.6° ± 8.0°. Thus, the PCBZL scaffold possessed the highest hydrophilicity, presumably because the urethane linkages on the side chains of the lysine moieties. In contrast, the benzyl groups on the side chains of PBG were hydrophobic, leading to this scaffold having the largest contact angle. The hydrophilicity of the 5CBZL5BG scaffold was between those of PBG and PCBZL, as expected because of the presence of equimolar amounts of BG and CBZL moieties in this copolypeptide. After partial hydrolysis of the 5CBZL5BG scaffold, the 5BL28-5BGA scaffold featured both positive and negative

**ADVANCED
SCIENCE NEWS**

www.advancedsciencenews.com

[M] acro-
olecular
Bioscience

www.mbs-journal.de

Figure 2. SEM images of various polypeptide fibrous scaffolds. A) PBG, B) PCBZL, C) 5CBZL5BG, and D) 5BL28-5BGA18. Magnification: 500×. Scale bar: 50 μm.
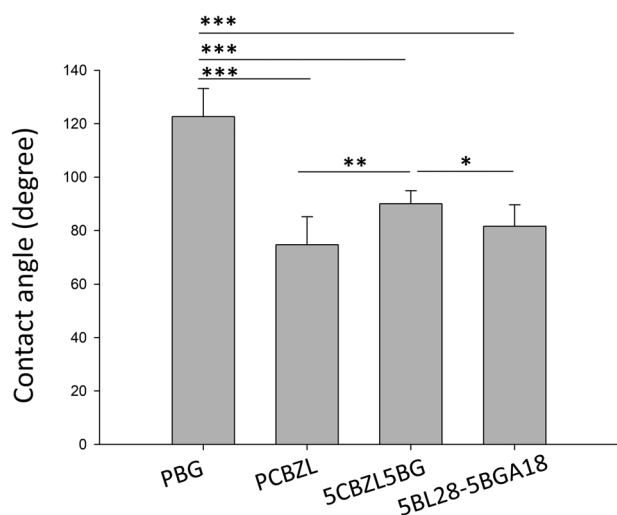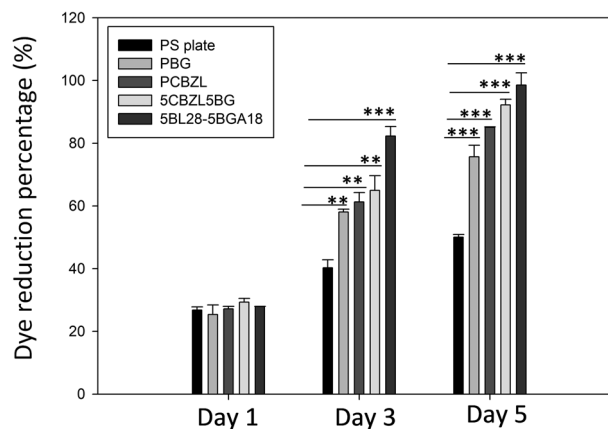

Figure 3. Water contact angle of various polypeptide scaffolds. $n = 3–5$. Statistical analysis was examined by Kruskal–Wallis H test (***$P < 0.001$, **$P < 0.01$, *$P < 0.05$).

Figure 4. Cell viability of PC-12 cells grown on different polypeptide scaffolds after 5-d culture. Each group was repeated three times. Statistical analysis was examined by Kruskal–Wallis H test (***$P < 0.001$, **$P < 0.01$, *$P < 0.05$).

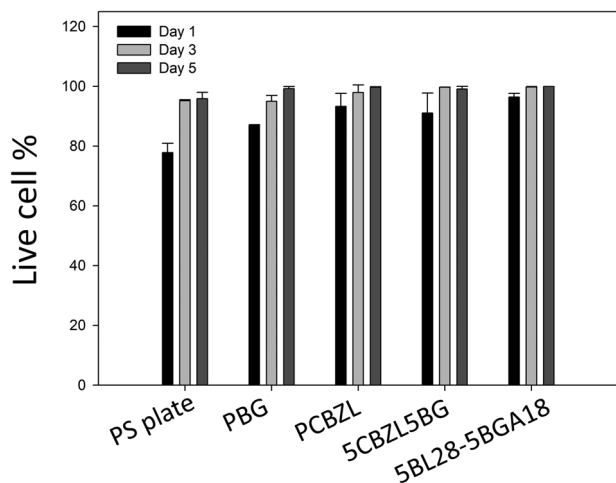charges, results in net positive charge with increased hydrophilicity and a lower contact angle.

3.3. Biocompatibility of Polypeptide Scaffolds

We used Alamar Blue and Live/Dead assays to investigate the biocompatibility of our polypeptide fibrous scaffolds. To evaluate the cell viability during the whole cell proliferation process, we performed the Alamar Blue assays on days 1, 3, and 5. The principle of this assay is to exploit the metabolic activity of cells

toward the dye Alamar Blue, with a lower dye concentration revealing higher cell viability. We used Equation (S2) (Supporting Information) to calculate the dye reduction percentage. We performed the cell culturing of all samples in a PS cell culture plate without any special cell adhesive coating. **Figure 4** reveals that all of the polypeptide scaffolds had cell viabilities superior to that of the PS culture plate. The cell counts on the various scaffolds all increased upon increasing the number of culturing days, implying that the scaffolds displayed good biocompatibility. After the first day, there were almost no differences in the activities of the PC-12 cells among the scaffolds; on the third day, however, the cell counts on the scaffolds were higher than on the

**ADVANCED
SCIENCE NEWS**

www.advancedsciencenews.com

⌈M⌉ acro-
olecular
Bioscience
www.mbs-journal.de

Figure 5. Live cell % of PC-12 cells after 1, 3, and 5-d culture on different polypeptide scaffolds. Cell count = 500–1000.

PS plate, with significantly higher cell counts on the scaffolds on the fifth day. Among the scaffolds, the PBG scaffold had the lowest cell viability, related to the better initial attachment ability of the PC-12 cells on the more hydrophilic lysine-containing PCBZL scaffold.[28] The 5CBZL5BG scaffold displayed both good cell adhesion from its hydrophilic lysine moieties and stimulated neurogenesis from its glutamate moieties; as a result, the cell viability of this co-polypeptide was better than that of its homo-polypeptides. The 5BL28-5BGA18 scaffold provided the best cell viability, due to its net positive charge favoring cell attachment and recognition, and its glutamic acid moieties favoring the stimulation of nerve growth and differentiation.[23]

We used a Live/Dead assay to evaluate the biocompatibility and biotoxicity of our scaffolds toward PC-12 cells. Figures S10 and S11 (Supporting Information) presents fluorescence staining images of PC-12 cells on the PS plate and our various scaffolds. The live cell populations on the scaffolds were significantly greater than that on the PS plate, while the red (dead) cells were almost invisible. The PC-12 cells grown on the 5BL28-5BGA18 scaffold had the highest cell population, consistent with our findings from the Alamar Blue cell viability tests. Moreover, the growth of the stained cells on the aligned scaffold was directional, suggesting that the aligned fibers in the scaffold could guide the direction of cell growth. We used the percentage of live cells as a representation of the number of live cells (**Figure 5**). After the first day of culturing, the percentage of live cells on the PS plate was lower than those on the polypeptide scaffolds, consistent with the latter having low cytotoxicity and good cell adhesion and viability. Notably, the percentages of live cells on every scaffold on the third and fifth days were all close 95%, possibly related to the removal of the detached dead cells after PBS washing on the first day.

Together with the results of the Alamar Blue assay, we conclude that the 5BL28-5BGA18 scaffold presenting glutamic acid and lysine moieties had the highest biocompatibility, due to of its net positive charge and hydrophilicity. A previous study found that biomaterials containing neurotransmitters could promote neuron cell viability, adhesion, and differentiation.[38] Because they are neurotransmitters, the glutamic acid moieties in the 5BL28-5BGA18 scaffold presumably also contributed to the high

biocompatibility. Together, our findings reveal that actual cellular outcomes were possible directly on the pristine polypeptide scaffold, without the need for pretreatment (e.g., use of a polylysine cell adhesion coating). Thus, our co-polypeptide scaffolds are unique in that they provide the dual functions of excellent cell adhesion and growth.

3.4. Neurite Outgrowth of Cells on Various Fibrous Polypeptide Scaffolds

Next, we studied the neurite outgrowth properties of PC-12 cells on our various scaffolds, with and without NGF. Figure S12 (Supporting Information) displays the results of fluorescence staining for PC-12 cell differentiation on the various scaffolds in the absence of NGF. No apparent neurite elongation occurred for any of the samples. After the addition of NGF, however, all of the samples displayed neurite outgrowth, with the neural activity and neurite length both being quite different among these scaffolds. The scaffolds containing glutamate moieties provided greater degrees of neurite growth in the presence of NGF. **Figure 6** reveals that the growth of elongated cells was aligned with the fiber direction of the scaffolds. **Figure 7** presents the neurite growth on the various scaffolds and the distributions of neurite lengths; **Figure 8** displays the lengths of the neurites; and **Figure 9** the neurite alignment. Table S2 (Supporting Information) summarizes the quantitative features. Figure 8 reveals that the neurite lengths followed the order PCBZL < PBG < 5CBZL5BG < 5BL28-5BGA18. Thus, the neurites on PBG were longer than those on PCBZL, due to the nerve stimulating function of the glutamate moieties. The neurites on the co-polypeptide were 32% longer than those on the homo-polypeptide scaffolds, consistent with the former scaffold providing good initial cell adhesion (from the lysine moieties) and effective neural stimulation (from the glutamate moieties). Among these scaffolds, 5BL28-5BGA18 displayed the longest neurites, arising from its glutamic acid and lysine moieties. Glutamic acid is a neurotransmitter that facilitates cell communication and brain neurogenesis.[22,23] Hence, we suspect that the cells could recognize the glutamic acid moieties on the polypeptide through direct contact. The glutamic acid moieties on the polypeptide chains of 5BL28-5BGA18 induced neurotransmitter-related cellular behavior to further enhance neurite outgrowth. 5BL28-5BGA18 is a net positively charged co-polypeptide that facilitates cell attachment and recognition simultaneously.

We investigated the capacity of the various fibrous scaffolds for cell differentiation with and without NGF treatment according to the literature.[39–41] We examined the levels of expression of the differentiated marker GAP43 in PC-12 cells (Figure S13, Supporting Information).The expression of GAP43 was upregulated under all of the conditions of culturing on the fibrous scaffolds, relative to that on the PS plate alone, whether treated with NGF (Figure S13A left panel and S13B, Supporting Information) or not (Figure S13A right panel and S13C, Supporting Information). We have examined the expression level of GAP43 in the presence and absence of the NGF group several times (Figure S14A,B, Supporting Information). In the absence of the NGF group, the expression of GAP43 has more variation than the presence of the NGF one. The protein expression on 5BL28-5BGA18
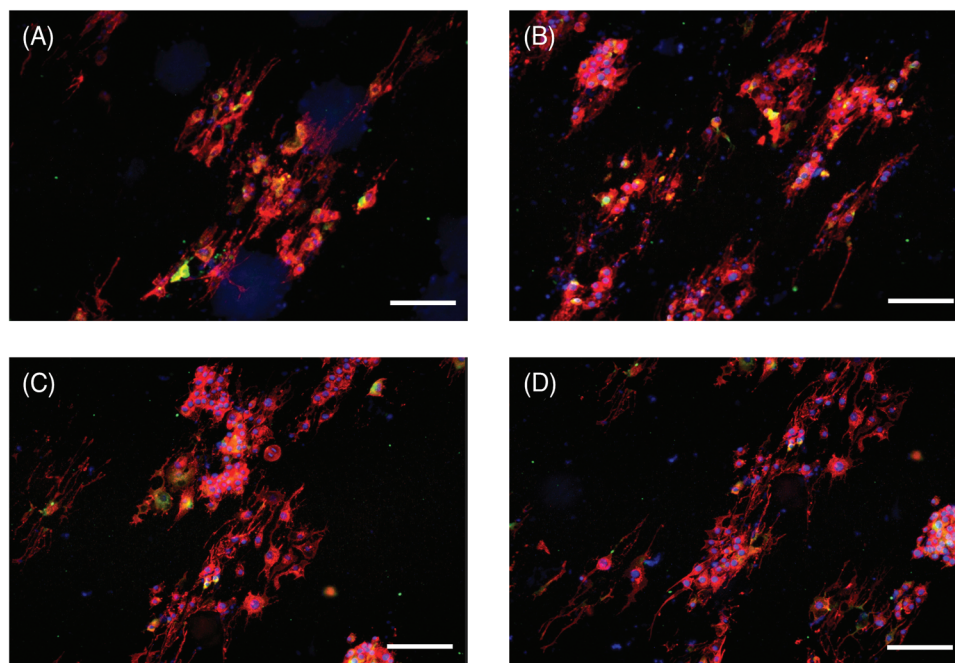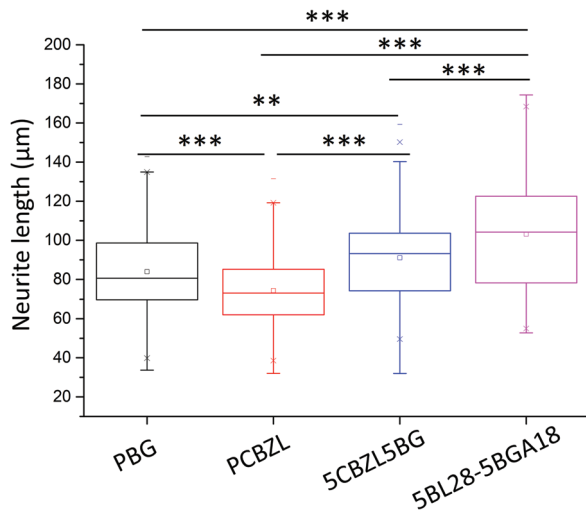
Figure 6. Fluorescence microscopic images of 5-day differentiated PC-12 cells on different polypeptide scaffolds containing aligned fibers: A) PBG, B) PCBZL, C) 5CBZL5BG, and D) 5BL28-5BGA18. Scale bar: 100 μm.
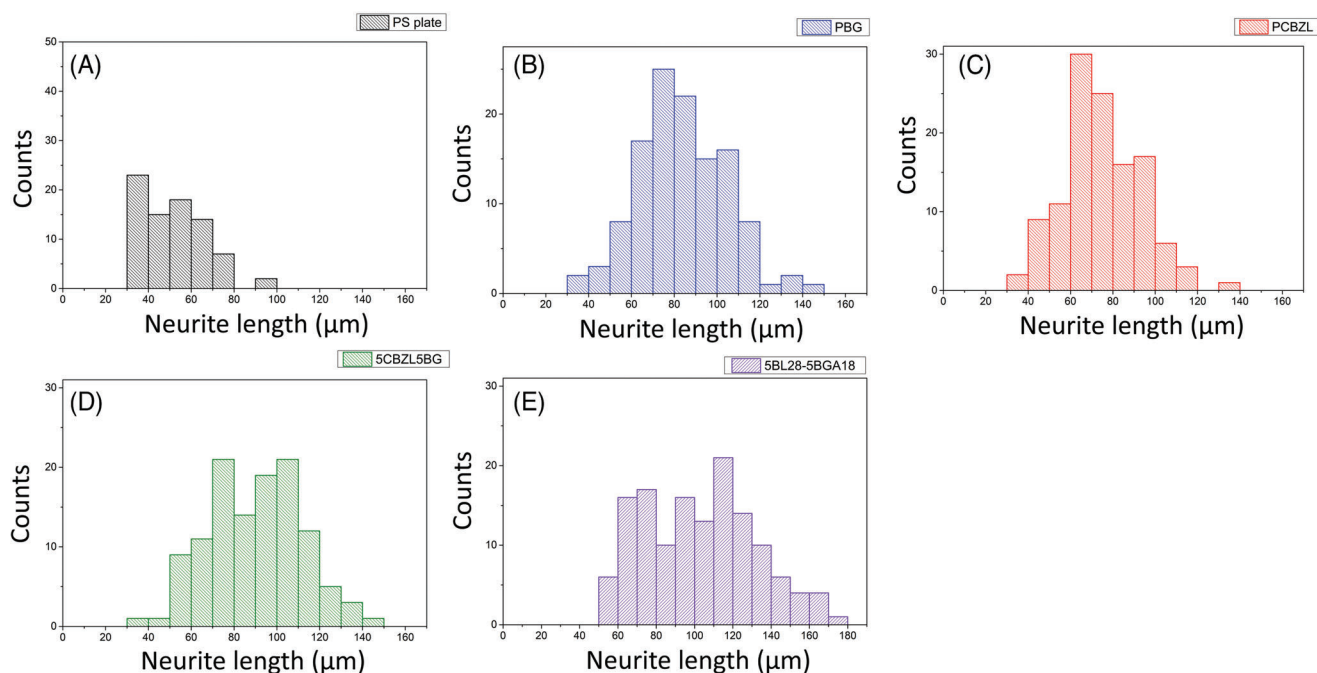
Figure 7. Distributions of PC-12 neurite lengths on different polypeptide scaffolds after 5-d differentiation: A) PS plate, B) PBG, C) PCBZL, D) 5CBZL5BG, and E) 5BL28-5BGA18. Neurite counts = 120 in each group.

(No NGF) shows a higher expression than other groups during these validations (Figure S14B, Supporting Information). In addition, we also verified another differentiated marker Synapsin1 in this validation (Figure S15, Supporting Information). Based on these preliminary data, the expression patterns of Synapsin1 were higher in the scaffolds group (with or without NGF treatment). Nonetheless, the antibody of anti-Synapsin1 has nonspecific bands around the predicted location on the western blot so we cannot judge it confidently. However, combined with the patterns of GAP43 expression analysis, we are certain that the PC-12

**ADVANCED
SCIENCE NEWS**

www.advancedsciencenews.com

**M acro-
olecular**
Bioscience
www.mbs-journal.de

Figure 8. Box chart of PC-12 neurite lengths on different polypeptide scaffolds after 5-d differentiation. Neurite counts = 120 for each group. Statistical analysis was examined by Kruskal–Wallis H test (***$P < 0.001$, **$P < 0.01$, *$P < 0.05$).

cells were more differentiated while being cultured on the fibrous scaffolds. Notably, the expression of GAP43 and Synapsin1 were dramatically upregulated under the NGF-treatment conditions, suggesting that the fibrous scaffolds displayed a synergistic effect with NGF in terms of the capacity of differentiation.

Directional outgrowth of neurites is important for neurons to transmit signals to their targets. Figure 9 provides a statistical analysis of the angle of alignment of the neurites. The aligned fibers clearly guided the directional outgrowth of the neurites. In contrast, the cells cultured on the PS plate extended their neurites in all direction. The neurite outgrowth was more aligned with the direction of the fibers when they contained glutamate moieties, as discussed earlier. Our findings confirm that glutamate provides a biological cue for neurite outgrowth, a feature desirable for neural tissue engineering.
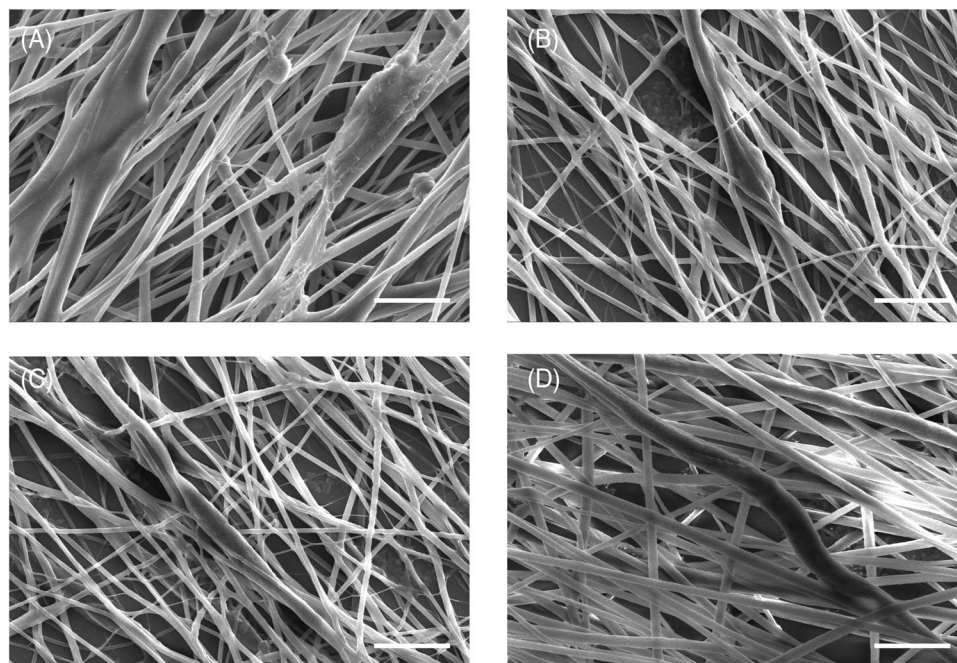
We used SEM to study the morphologies of the neurite outgrowth on the various scaffolds featuring aligned fibers. The neurites grew along and in alignment with the fibers of these scaffolds, as evidenced in both fluorescent microscopy (Figure 6) and SEM (**Figure 10**) images. The cells grew not only on the scaffold surfaces but also within the scaffolds, through the pores of the 3D fibrous structures.

4. Conclusions

We have synthesized dual-function co-polypeptides containing glutamate and lysine moieties and fabricated them into 3D scaffolds with aligned fibers. We also prepared PBG and PCBZL homo-polypeptides for comparison and used a PS plate as a control. We installed net positive charge into the co-polypeptide scaffold through partial hydrolysis of a preformed scaffold, without affecting its physical integrity. All four polypeptides examined in this study exhibit good biocompatibility and no cytotoxicity. The co-polypeptide scaffolds containing both glutamate and lysine moieties exerted their functions effectively, with both good cell attachment and good cell viability. In particular, the net positively charged co-polypeptide fibrous scaffold displayed the best cell performance, as well as the best neurite outgrowth (32% increase in neurite length). This behavior was due to the positively charged lysine moiety providing high cell affinity, attachment, growth,
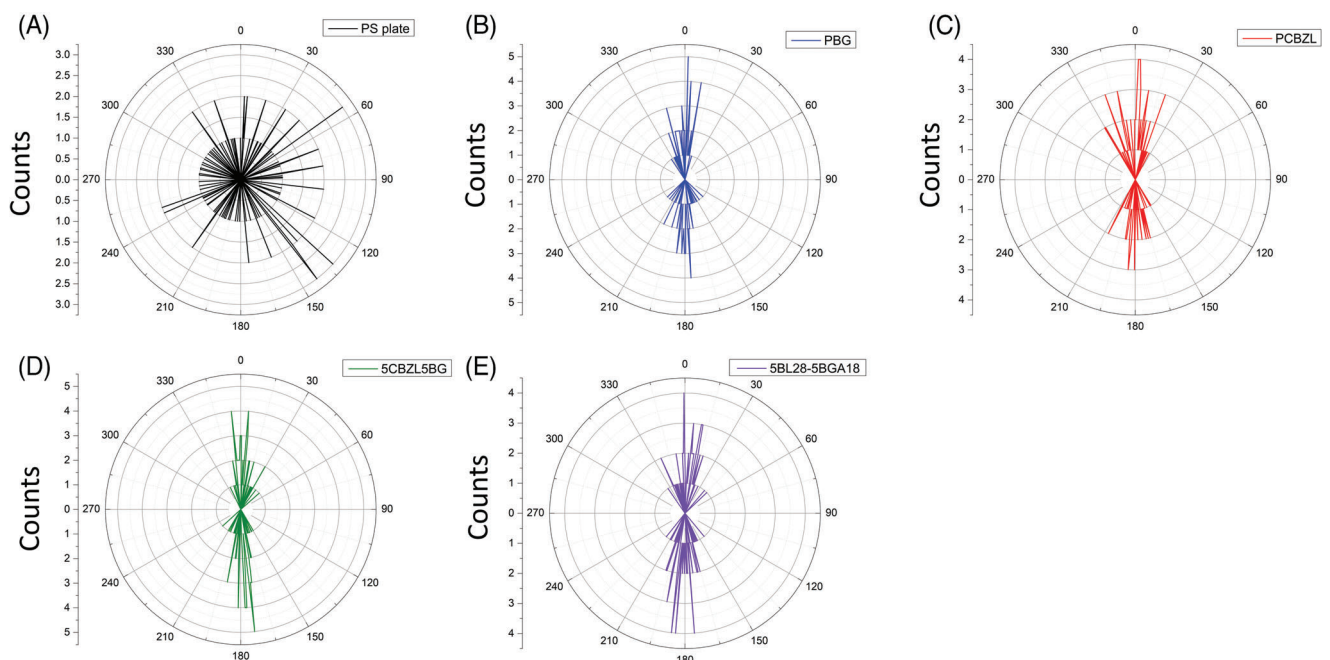
Figure 9. Neurite orientation of 5-d differentiated PC-12 cells on A) PS plate, B) PBG, C) PCBZL, D) 5CBZL5BG, and E) 5BL28-5BGA18. Neurite counts = 120 in each group.

**ADVANCED
SCIENCE NEWS**

www.advancedsciencenews.com

M acro-
olecular
Bioscience

www.mbs-journal.de

Figure 10. SEM images of 5-d differentiated neurites of PC-12 cells on polypeptide scaffolds with aligned fibers: A) PBG, B) PCBZL, C) 5CBZL5BG, and D) 5BL28-5BGA18. Scale bar: 100 μm.

and differentiation, while the glutamic acid moiety enhanced the degrees of cell recognition and neurite growth through neural simulation. From experiments quantifying the degrees of neural cell differentiation, we found that the differentiation of PC-12 cells when cultured on the fibrous scaffolds was higher than that on the PS plate, and that the expression of GAP43 was increased under the conditions of NGF treatment. Furthermore, the co-polypeptide scaffold could be used directly as a cell culture carrier, without any cell adhesion pretreatment, thereby shortening the cell culture time and minimizing experimental errors. To the best of our knowledge, this paper is the first to demonstrate that dual-function co-polypeptide fibrous scaffolds containing aligned fibers can provide high rates of neurite growth and alignment, with potential for application in neural tissue engineering.

Supporting Information

Supporting Information is available from the Wiley Online Library or from the author.

Acknowledgements

Conflict of Interest

The authors declare no conflict of interest.

Data Availability Statement

The data that support the findings of this study are available in the Supporting Information of this article.

Keywords

[1] G. Ciardelli, V. Chiono, *Macromol. Biosci.* **2006**, *6*, 13.
[2] M. Keshavarz, D. J. Wales, F. Seichepine, M. E. M. K. Abdelaziz, P. Kassanos, Q. Li, B. Temelkuran, H. Shen, G.-Z. Yang, *Biomed. Mater.* **2020**, *15*, 055011.
[3] R. A. Koppes, S. Park, T. Hood, X. Jia, N. Abdolrahim Poorheravi, A. H. Achyuta, Y. Fink, P. Anikeeva, *Biomaterials* **2016**, *81*, 27.
[4] W. Z. Ray, S. E. Mackinnon, *Exp. Neurol.* **2010**, *223*, 77.
[5] A. Mobasseri, A. Faroni, B. M. Minogue, S. Downes, G. Terenghi, A. J. Reid, *Tissue Eng., Part A* **2015**, *21*, 1152.
[6] T. B. Alma, C. S. Iwuji, N. C. Iheaturu, *J. Chem. Pharm. Res.* **2019**, *11*, 1.
[7] D. Walma, K. M. Yamada, *Development* **2020**, *147*, 175596.
[8] W. Xue, W. Shi, Y. Kong, M. Kuss, B. Duan, *Bioact. Mater.* **2021**, *6*, 4141.
[9] T. J. Deming, *Prog. Polym. Sci.* **2007**, *32*, 858.
[10] K. Numata, *Polym. J.* **2015**, *47*, 537.
[11] R. Bucci, E. Georgilis, A. M. Bittner, M. L. Gelmi, F. Clerici, *Nanomaterials* **2021**, *11*, 1262.
[12] F. Zha, W. Chen, L. Zhang, D. Yu, *J. Biomater. Sci., Polym. Ed.* **2020**, *31*, 519.

[13] B. Cao, J. Yin, S. Yan, L. Cui, X. Chen, Y. Xie, *Macromol. Biosci.* **2011**, *11*, 427.

[14] M. Rad-Malekshahi, L. Lempsink, M. Amidi, W. E. Hennink, E. Mastrobattista, *Bioconjugate Chem.* **2016**, *27*, 3.

[15] J. Ding, C. Xiao, X. Zhuang, C. He, X. Chen, *Mater. Lett.* **2012**, *73*, 17.

[16] D. Srinath, S. Lin, D. K. Knight, A. S. Rizkalla, K. Mequanint, *J. Tissue Eng. Regener. Med.* **2014**, *8*, 578.

[17] L. J. Del Valle, M. Roa, A. Díaz, M. T. Casas, J. Puiggalí, A. Rodríguez-Galán, *J. Polym. Res.* **2012**, *19*, 9792.

[18] Z.-H. Wang, Y.-Y. Chang, J.-G. Wu, C.-Y. Lin, H.-L. An, S.-C. Luo, T. K. Tang, W.-F. Su, *Macromol. Biosci.* **2018**, *18*, 1700251.

[19] J. Qian, X. Yong, W. Xu, X. Jin, *Mater. Sci. Eng., C* **2013**, *33*, 4587.

[20] S. Bu, S. Yan, R. Wang, P. Xia, K. Zhang, G. Li, J. Yin, *ACS Appl. Mater. Interfaces* **2020**, *12*, 12468.

[21] T.-C. Chen, P.-Y. She, D. F. Chen, J.-H. Lu, C.-H. Yang, D.-S. Huang, P.-Y. Chen, C.-Y. Lu, K.-S. Cho, H.-F. Chen, W.-F. Su, *Int. J. Mol. Sci.* **2019**, *20*, 178.

[22] M. Song, S. P. Yu, O. Mohamad, W. Cao, Z. Z. Wei, X. Gu, M. Q. Jiang, L. Wei, *Neurobiol. Dis.* **2017**, *98*, 9.

[23] C.-Y. Lin, S.-C. Luo, J.-S. Yu, T.-C. Chen, W.-F. Su, *ACS Appl. Bio Mater.* **2019**, *2*, 518.

[24] T.-L. Ma, S.-C. Yang, T. Cheng, M.-Y. Chen, J.-H. Wu, S.-L. Liao, W.-L. Chen, W.-F. Su, *J. Mater. Chem. B* **2022**, *10*, 6372.

[25] W.-H. Lee, C.-Y. Loo, W. Chrzanowski, R. Rohanizadeh, *J. Biomed. Mater. Res., Part A* **2015**, *103*, 2150.

[26] T. Elakkiya, R. Sheeja, K. Ramadhar, T. S. Natarajan, *J. Appl. Polym. Sci.* **2013**, *128*, 2840.

[27] D. B. Khadka, D. T. Haynie, *ACS Appl. Mater. Interfaces* **2010**, *2*, 2728.

[28] H. Yoshida, D. Klee, M. Möller, M. Akashi, *Adv. Funct. Mater.* **2014**, *24*, 6359.

[29] T. Ma, C. Tsai, S. Luo, W. Chen, Y. Huang, W. Su, *React. Funct. Polym.* **2022**, *175*, 105265.

[30] H. Liu, X. Zhang, Z. Zhao, F. Yang, R. Xue, L. Yin, Z. Song, J. Cheng, S. Luan, H. Tang, *Biomater. Sci.* **2021**, *9*, 2721.

[31] M. Piatkovsky, H. Acar, A. B. Marciel, M. Tirrell, M. Herzberg, *J. Membr. Sci.* **2018**, *549*, 507.

[32] Y. Zhang, W. Song, I. Kim, *J. Nanosci. Nanotechnol.* **2020**, *20*, 6968.

[33] Y. Huang, Z. Tang, X. Zhang, H. Yu, H. Sun, X. Pang, X. Chen, *Biomacromolecules* **2013**, *14*, 2023.

[34] E. P. Shen, M.-R. Chen, W.-L. Chen, H.-S. Chu, K.-L. Chen, F.-R. Hu, *Ocul. Immunol. Inflammation* **2020**, *28*, 876.

[35] P. H. Chen, H. C. Liao, S. H. Hsu, R. S. Chen, M. C. Wu, Y. F. Yang, C. C. Wu, M. H. Chen, W. F. Su, *RSC Adv.* **2015**, *5*, 6932.

[36] L. Bacakova, E. Filova, M. Parizek, T. Ruml, V. Svorcik, *Biotechnol. Adv.* **2011**, *29*, 739.

[37] D. P. Dowling, I. S. Miller, M. Ardhaoui, W. M. Gallagher, *J. Biomater. Appl.* **2011**, *26*, 327.

[38] Z. Zhou, P. Yu, H. M. Geller, C. K. Ober, *Biomaterials* **2012**, *33*, 2473.

[39] S. H. Bhang, S. I. Jeong, T.-J. Lee, I. Jun, Y. B. Lee, B.-S. Kim, H. Shin, *Macromol. Biosci.* **2012**, *12*, 402.

[40] X. Su, Y. Huang, R. Chen, Y. Zhang, M. He, X. Lu, *Regener. Biomater.* **2021**, *8*, rbab031.

[41] Y. Yu, X. Lü, F. Ding, *J. Biomed. Nanotechnol.* **2015**, *11*, 816.